Characterizing Biomass Feedstock Transport Properties Using State of the Art Imaging and Computational Techniques

Meagan F. Crowley[1], Hariswaran Sitaraman[2], Jordan Klinger[3], Francois Usseglio-Viretta[4], Nicholas E. Thornburg[5], Nick Brunhart-Lupo[2], M. Brennan Pecha[1], Yidong Xia[3], and Peter N. Ciesielski[1]

1. Renewable Resources and Enabling Sciences Center, National Renewable Energy Laboratory, Golden, Colorado, USA, 2. Computational Science Center, National Renewable Energy Laboratory, Golden, Colorado, USA, 3. Energy Environment Science & Technology Directorate, Idaho National Laboratory, Idaho Falls, Idaho, USA, 4. Center for Energy Conversion & Storage Systems, National Renewable Energy Laboratory, Golden, Colorado, USA, 5. Center for Integrated Mobility Sciences, National Renewable Energy Laboratory, Golden, Colorado, USA

FEEDSTOCK-CONVERSION INTERFACE CONSORTIUM

NREL/PO-2800-83182

Abstract

The microstructure of lignocellulosic biomass determines heat and mass transfer during conversion processes. We present a novel method for characterizing the transport properties of biomass using advanced imaging and computational techniques. The microstructure of two woody feedstocks, red oak and Douglas fir, before and after pyrolysis, is revealed using X-ray computed tomography (XCT). Transport properties are calculated from the XCT images, and principal permeability tensors are calculated using an immersed boundary-based finite volume solver to model gas flow through the geometries. We observe that the permeabilities of native biomass are distinctly anisotropic, however, this anisotropy is greatly reduced after pyrolysis.

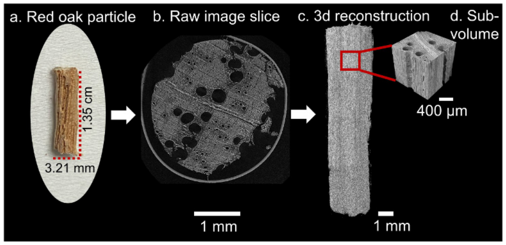

Figure 1. Diagram of XCT workflow. (a) Initial particle, native red oak photograph. (b) Raw image slice from XCT radiograph. (c) 3D reconstruction of the full particle from the raw images. (d) Cropped sub-volume used for numerical analysis and calculation of material properties.

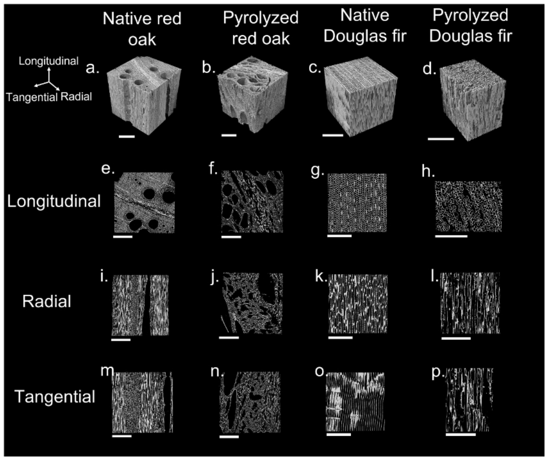

Figure 2. Sub-volumes of each sample with longitudinal, radial, and tangential slices. (a) Native red oak sub-volume, (b) Pyrolyzed red oak sub-volume, (c) Native Douglas fir sub-volume, (d) Pyrolyzed Douglas fir sub-volume, Longitudinal slices of (e) Native red oak, (f) Pyrolyzed red oak, (g) Native Douglas fir, (h) Pyrolyzed Douglas fir, Radial slices of (i) Native red oak, (j) Pyrolyzed red oak, (k) Native Douglas fir, (l) Pyrolyzed Douglas fir, Tangential slices of (m) Native red oak, (n) Pyrolyzed red oak, (o) Native Douglas fir, (p) Pyrolyzed Douglas fir. All scale bars indicate 400µm length.

Presented at the 2022 FCIC Annual Meeting June 9th, 2022

Methods

- ***3D pore microstructure of native and pyrolyzed red oak and Douglas fir imaged using X-ray Computed tomography and software reconstruction***
- ***1mm^3 sub-volumes imported into Mesoflow, a compressible finite-volume solver developed on the AMReX library. (Zhang et al, 2019) for CFD simulations***
- ***Permeability was computed from simulations using the Navier-Stokes momentum balance:***

$$\frac{\partial\rho}{\partial t}+\frac{\partial(\rho U_i)}{\partial x_i}=0 \quad (1)$$

$$\frac{\partial(\rho U_i)}{\partial t}+\frac{\partial}{\partial x_j}\left(\rho U_i U_j\right)=-\frac{\partial P}{\partial x_i}+\frac{\partial\tau_{ij}}{\partial x_j} \quad (2)$$

$$\frac{\partial(\rho e)}{\partial t}+\frac{\partial}{\partial x_i}(\rho e+P)=\frac{\partial}{\partial x_i}\left(k\frac{\partial T}{\partial x_i}\right)+\frac{\partial\,(\tau_{ij}v_j)}{\partial x_i} \quad (3)$$

- ***The equations are closed using ideal gas law, total energy, and Newtonian fluid assumption:***

$$P=\rho RT \quad (4)$$

$$\rho e=\frac{P}{\gamma-1}+\frac{1}{2}\rho U_i U_i \quad (5)$$

$$\tau_{ij}=\mu\left(\frac{\partial U_j}{\partial x_i}+\frac{\partial U_i}{\partial x_j}\right)-\frac{2}{3}\mu\frac{\partial U_k}{\partial x_k}\,\delta_{ij} \quad (6)$$

- ***Permeability is calculated using Darcy's law:***

$$\mathrm{K_i}=\bar{\mathrm{U}}_\mathrm{i}\mu\left(\overline{\frac{\partial \mathrm{P}}{\partial \mathrm{x_i}}}\right)^{-1} \quad (7)$$

- ***Void fraction, tortuosity calculated using the open-source software tool MATBOX :***

$$\varepsilon_k=\frac{1}{N}\sum_{i=1}^{N}v(i),\text{with } v(i)=\begin{cases}1\ if\ v(i)\in \text{ phase } k\\ 0\ if\ v(i)\notin \text{ phase } k\end{cases} \quad 8)$$

- ***The tortuosity, τ, along direction i is solved for according to Equation 9:***

$$\frac{D_{eff,i}}{D_{bulk}}=\frac{\varepsilon}{\tau_i} \quad (9)$$

Table 1. Calculated permeability tensors for each sample. All values in units of m^2.

Direction	Native red oak Calculated	Literature range red oak (0% moisture) (Choong et al., 1974)	Pyrolyzed red oak Calculated	Native Douglas fir Calculated	Literature range Douglas fir/Pine (5-9% moisture) (Comstock, 1970)	Pyrolyzed Douglas fir Calculated
Longitudinal	8.76E-12	9.6E-12 to 6E-11	9.13E-12	1.36E-12	9E-13 to 3 E-11	2.81E-12
Radial	3.64E-15	8E-16 to 3.5E-15	3.35E-13	1.81E-14	8E-17 to 2E-15	2.29E-13
Tangential	1.30E-15	4.5E-16 to 1.3E-15	8.98E-13	3.46E-16	1E-17 to 1E-15	1.32E-13

Table 2. Calculated void fraction, directional tortuosity factors of the void phase, and directional effective diffusivity multipliers of each species before and after pyrolysis.

Property	Native red oak	Pyrolyzed red oak	Native Douglas fir	Pyrolyzed Douglas fir
Void Fraction	0.71	0.87	0.66	0.77
Longitudinal tortuosity factor	1.13	1.16	1.26	1.08
Radial tortuosity factor	2.47	1.29	16.7	1.99
Tangential tortuosity factor	6.00	1.39	38.5	4.02
Longitudinal effective diffusivity multiplier	0.62	0.75	0.52	0.71
Radial effective diffusivity multiplier	0.29	0.67	0.04	0.38
Tangential effective diffusivity multiplier	0.12	0.62	0.02	0.19

Results & Discussion

- ***Microstructure is species-specific (Ciesielski et al 2015)***
  - ***Native red oak = fine pore structure of fiber cells with large-diameter vessel cell channels characteristic of hardwoods***
  - ***Native Douglas fir = highly regular pore structure with arrays of axial tracheids characteristic of softwoods.***
- ***Longitudinal direction is the dominant avenue for mass and heat transport in both native Douglas fir and red oak samples***
  - ***highest permeability and lowest tortuosity = path of least resistance***
- ***Thermal treatment affects microstructure of both species:***
  - ***pore structure degrades***
  - ***void volume increases***
  - ***directional anisotropy reduces***
- ***These trends are reflected in the reduction in the directional anisotropy for void fraction, tortuosity, and permeability in both Douglas fir and Native oak samples.***
- ***The values for permeability, tortuosity, and void fraction can be a useful touchstone for the biorefining community to improve the fidelity of conversion models by explicitly including species-specific transport properties.***

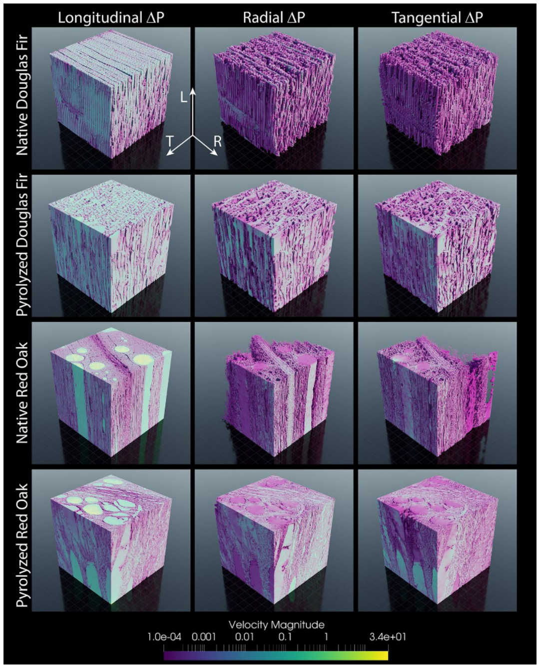

Figure 3. Steady state visualizations of permeability simulations for native and pyrolyzed Douglas fir and red oak XCT sub-volumes. In each case, pressure gradients were applied to only one of the longitudinal, radial, or tangential directions. Velocity magnitudes below 10^{-4} are not visualized, hence the partial renditions for native red oak in the radial and tangential directions.

References:

Choong, E., Tesoro, F., and Manwiller, F. (1974). Permeability of twenty-two small diameter hardwoods growing on southern pine sites. Wood and Fiber 6 (1): 91-101.

Ciesielski, P.N., Crowley, M.F., Nimlos, M.R., Sanders, A.W., Wiggins, G.M., Robichaud, D., et al. (2015). Biomass Particle Models with Realistic Morphology and Resolved Microstructure for Simulations of Intraparticle Transport Phenomena. Energy & Fuels 29(1), 242-254. doi: 10.1021/ef502204v.

Comstock, G.L. (1970). Directional permeability of softwoods. Wood and Fiber Science 1(4), 283-289.

Usseglio-Viretta, F.L.E., Patel, P., Bernhardt, E., Mistry, A., Mukherjee, P.P., Allen, J., et al. (2022). MATBOX: An Open-source Microstructure Analysis Toolbox for microstructure generation, segmentation, characterization, visualization, correlation, and meshing. SoftwareX 17, 100915. doi: https://doi.org/10.1016/j.softx.2021.100915

Zhang, W., Almgren, A., Beckner, V., Bell, J., Blaschke, J., Chan, C., et al. (2019). AMReX: a framework for block-structured adaptive mesh refinement. Journal of Open Source Software 4(37), 1370-1370.

This work was authored under the Feedstock Conversion Interface Consortium for the U.S. Department of Energy (DOE). Funding provided by U.S. Department of Energy Office of Energy Efficiency and Renewable Bioenergy Technologies Office. The views expressed in the article do not necessarily represent the views of the DOE or the U.S. Government. The U.S. Government retains and the publisher, by accepting the article for publication, acknowledges that the U.S. Government retains a nonexclusive, paid-up, irrevocable, worldwide license to publish or reproduce the published form of this work, or allow others to do so, for U.S. Government purposes.